Available online at www.sciencedirect.com
SCIENCE DIRECT®
Physics of the Earth and Planetary Interiors 138 (2003) 231–239
PHYSICS OF THE EARTH AND PLANETARY INTERIORS
www.elsevier.com/locate/pepi

Relocation of the 26 July 2001 Skyros Island (Greece) earthquake sequence using the double-difference technique

Zafeiria Roumelioti [a], Anastasia Kiratzi [a,*], Nikos Melis [b]

[a] *Department of Geophysics, Aristotle University of Thessaloniki, P.O. Box 352-1, 54124 Thessaloniki, Greece*
[b] *Institute of Geodynamics, National Observatory of Athens, P.O. Box 20048, 11810 Athens, Greece*

Received 25 October 2002; received in revised form 27 May 2003; accepted 12 June 2003

Abstract

Routine catalog phase data from the permanent stations of the Greek National Seismological Network were used to relocate 445 aftershocks of the 26 July 2001 ***M*** 6.5 Skyros (North Aegean Sea) earthquake, using the double-difference (DD) algorithm of Waldhauser and Ellsworth [Bull. Seism. Soc. Am. 19 (2000) 1353]. The relocated epicenters define two zones: (a) a main NW–SB cluster of ∼27 km length and (b) a secondary less pronounced NE–SW cluster of ∼15 km length, which was activated within 24 h after the mainshock occurrence. Redistribution of stresses due to the occurrence of the mainshock certainly played a role in this activation. The Skyros mainshock occurred in a region controlled by the activity of the Aegean Sea strands of the dextral strike-slip North Anatolian Fault (NAF). The main aftershock zone is almost perpendicular to the main tectonic NAF strands, and confirms that the causative fault strikes NW–SE associated with sinistral strike-slip motion. The 2001 Skyros earthquake is the first instrumentally recorded event that indicates re-activation of the old tectonic NW–SE trending structures of continental Greece under the presently acting stress field in a way sketched by Kiratzi [Geophys. J. Int. 151 (2002) 360].

Keywords: Epicentre relocation; Aegean Sea; Skyros earthquake

1. Introduction

On 26 July 2001 (00:21:38.18 UTC) an earthquake with epicentral coordinates 38.99°N, 24.36°E, depth ∼13 km, and moment magnitude, ***M*** 6.5 occurred near the Greek island of Skyros in the North Aegean Sea. Approximately 90 houses were damaged, mostly old traditional dwellings in the capital of Skyros. Among them, the almost 1000-year-old monastery of St. George the Arab, situated inside the castle, was badly damaged. Although the earthquake caused this limited damage to the nearby Skyros Island, it is considered to be of great scientific significance. This stems from the fact that even though the area of occurrence is known for its dextral strike-slip faults, related to the continuation of the North Anatolia Fault Zone into the North Aegean Sea (e.g. Papazachos et al., 1984; Rocca et al., 1985; Kiratzi et al., 1991; Papadimitriou and Sykes, 2001), this earthquake provided for the first time recorded evidence for sinistral strike-slip faulting in a direction perpendicular to the main tectonic lines (Melis et al., 2001; Benetatos et al., 2002; Drakatos et al., 2002; Karakostas et al., 2003; Kiratzi, 2002; Roumelioti et al., 2003; Papadopoulos et al., 2002; Zahradnik, 2002). The general picture of the area of the 2001 Skyros mainshock is shown in Fig. 1.

The aim of the present study is to relocate the epicentres of the 2001 Skyros sequence in order to obtain

* Corresponding author. Tel.: +30-310-998486; fax: +30-310-998528.
E-mail address: kiratzi@geo.auth.gr (A. Kiratzi).

0031-9201/$ – see front matter © 2003 Elsevier B.V. All rights reserved.
doi:10.1016/S0031-9201(03)00138-9

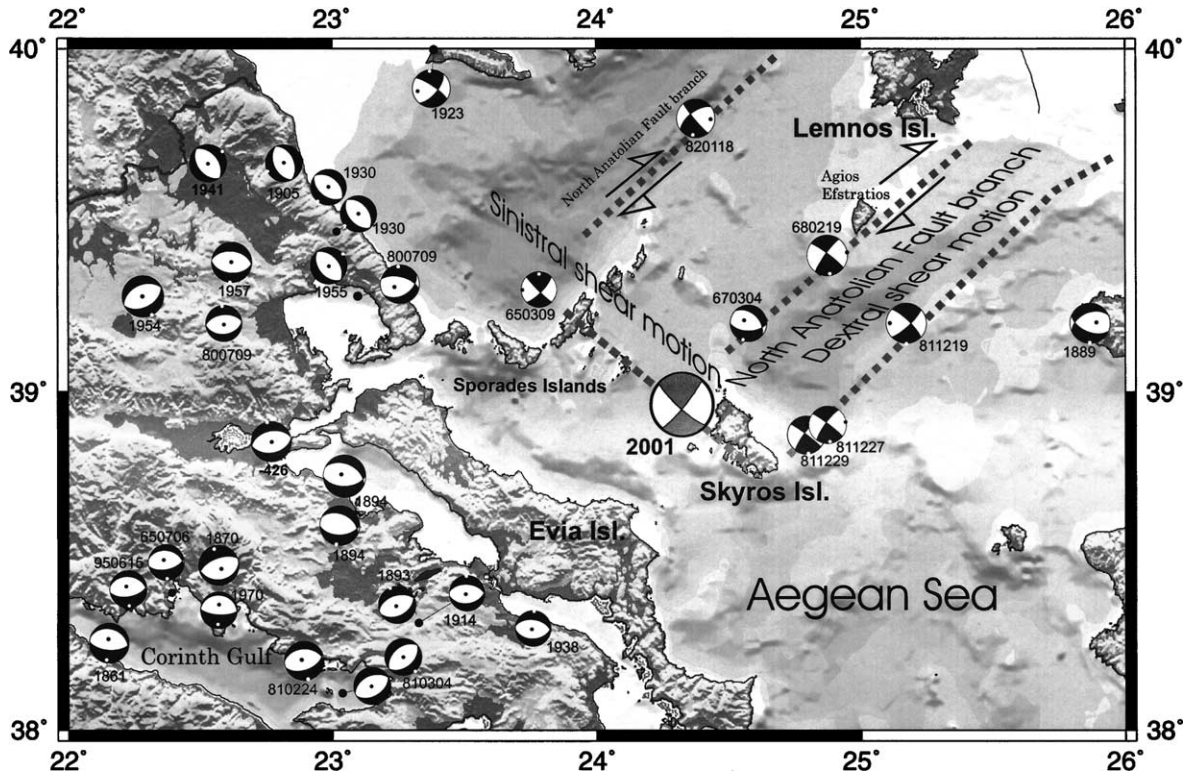

Fig. 1. Earthquake focal mechanisms of previous events of the broader area. For the focal mechanisms of historical events and events prior to 1964 data from field observations and macroseismic data (Papazachos and Papazachou, 1997) are used to hypothesize the mechanism. The rest mechanisms are from Papazachos et al. (1998) and Louvari (2000). The mechanism for the 2001 Skyros mainshock is from Benetatos et al. (2002). The corresponding year or full date (yymmdd) of occurrence is indicated next to each focal mechanism.

an enhanced picture of the seismicity distribution. Even though routinely determined epicentres are capable of revealing the rough picture of the seismicity, they are not suitable for studies of the fine structure of the causative faults, as their location uncertainties are sometimes larger than the source dimension itself. In Greece, the average uncertainties in the catalogue hypocenter locations are of the order of 12 km in the horizontal (ERH) and 3 km in the vertical (ERZ) direction (Skarlatoudis, 2002). Better accuracy in the hypocentral parameters is also required for more detailed studies, like the slip distribution on the fault plane (Roumelioti et al., 2003).

The relocation algorithm (HypoDD code) that we apply is based on the double-difference (DD) technique (Waldhauser and Ellsworth, 2000; Waldhauser, 2001). The DD technique belongs to the relative earthquake location methods (e.g. Fréchet, 1985; Got et al., 1994), which take advantage of the fact that if the hypocentral separation between two earthquakes is small enough compared to the event–station distance and the scale length of velocity heterogeneity, then the ray paths can be considered identical along their entire length. Under this assumption, the differences in the travel times for two earthquakes recorded at the same station can be attributed to differences in their hypocenter spatial separation. In this way, errors due to inaccurately modeled velocity structure, especially those related to the structure beneath the recording station, are minimized without the use of station corrections. Therefore, the technique can be particularly effective for tectonically complex areas, such as the Aegean Sea, where inaccurately modeled velocity structure can introduce significant errors into the theoretically estimated travel times.

2. Data

The input data for the double-difference earthquake location algorithm consist of catalogue P- and S-wave arrival times. We used the arrival times at the stations of two permanent networks in Greece (Fig. 2) operated by the Geodynamic Institute of the National Observatory of Athens and the Department of Geophysics of the Aristotle University of Thessaloniki.

Phase data from the two networks were combined for all earthquakes recorded within the first 5 weeks after the Skyros mainshock (27 July to 31 August 2001). From the original data set, we chose only those earthquakes for which 10 or more phases were available. Our final data set consists of 8909 P- and S-wave arrival times, corresponding to 570 earthquakes. The selected phases were subsequently used to estimate P- and S-wave differential travel times relative to the routinely calculated origin times of the earthquakes.

3. Method used

The DD technique is thoroughly described in Waldhauser and Ellsworth (2000) and only a general outline is given here. The technique has the capability of incorporating travel time differences formed from catalogue phases and/or inferred from cross-spectral methods. Theoretical travel time differences are also calculated based on a simple 1D P-velocity model, input by user, and the residuals between theoretical

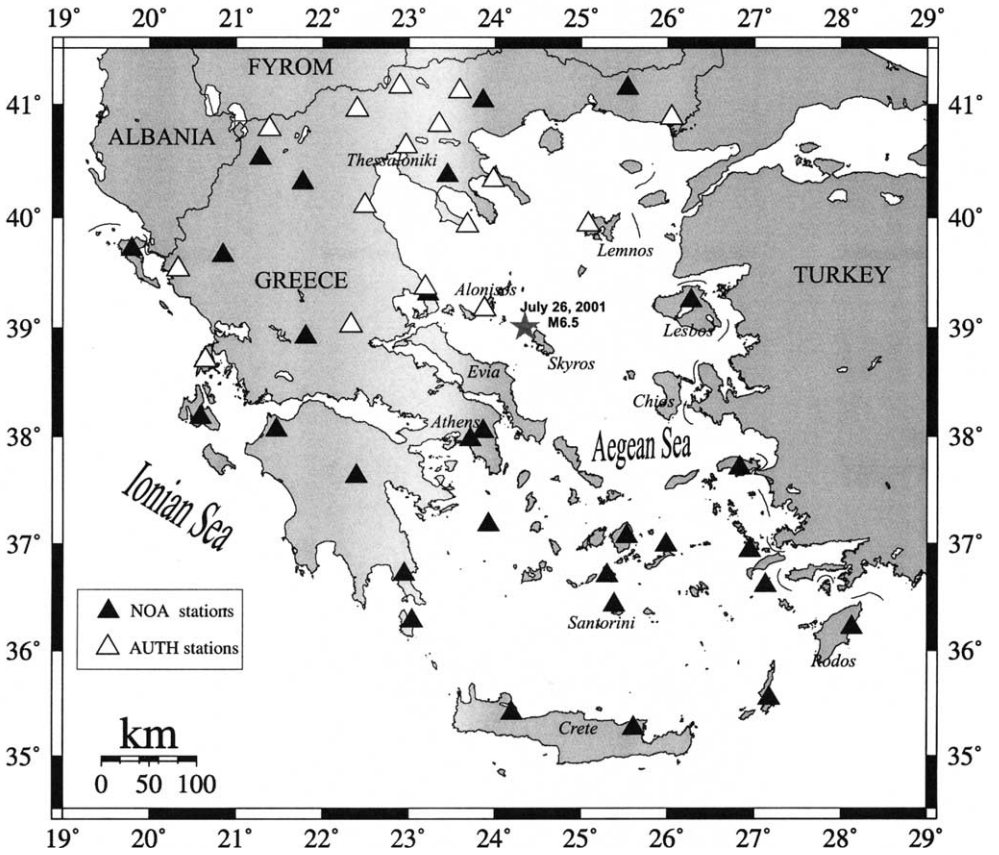

Fig. 2. Regional map showing locations of the permanent stations operated by the National Observatory of Athens (black triangles) and by the Geophysical Laboratory of the Aristotle University of Thessaloniki (white triangles). The star symbol corresponds to the epicenter of the 2001 Skyros mainshock.

and observed times are minimized in an iterative procedure.

In the general case where two events are close to each other compared to the event–station distance and to the scale of velocity heterogeneity in the broader hypocentral area, the residual between observed and calculated differential travel time for the two events can be calculated as:

$$dr_k^{ij} = (t_k^i - t_k^j)^{obs} - (t_k^i - t_k^j)^{cal} \quad (1)$$

where t is the travel time, superscripts i and j correspond to the two different events and subscript k corresponds to a particular observation (e.g. one particular phase to one common station). The first term of the right part of the above equation corresponds to the observed (obs) differential travel time of the two events, while the second term corresponds to the difference in their theoretical (cal) travel time.

The double-difference equations are derived from differencing Geiger's equation for earthquake location (Geiger, 1910) and have the form:

$$\frac{\partial t_k^i}{\partial \boldsymbol{m}} \Delta \boldsymbol{m}^i - \frac{\partial t_k^j}{\partial \boldsymbol{m}} \Delta \boldsymbol{m}^j = dr_k^{ij} \quad (2)$$

where $\Delta \boldsymbol{m}$ (Δx, Δy, Δz, $\Delta \tau$) is the change in the four hypocentral parameters of the events. The above equation can be expanded as:

$$\frac{\partial t_k^i}{\partial x} \Delta x^i + \frac{\partial t_k^i}{\partial y} \Delta y^i + \frac{\partial t_k^i}{\partial z} \Delta z^i + \Delta \tau^i - \frac{\partial t_k^j}{\partial x} \Delta x^j - \frac{\partial t_k^j}{\partial y} \Delta y^j - \frac{\partial t_k^j}{\partial z} \Delta z^j - \Delta \tau^j = dr_k^{ij} \quad (3)$$

This equation relates the residual, dr, between observed and theoretical travel time difference between the two events (Eq. (1)) to changes in each event's locations (x, y, z) and origin time (τ).

In the double-difference earthquake location method, the partial derivatives in Eq. (3) are estimated for each event pair–station combination, and the resulting equations build up a system of linear equations of the form:

$$\boldsymbol{W}\boldsymbol{G}\boldsymbol{m} = \boldsymbol{W}\boldsymbol{d} \quad (4)$$

where $\boldsymbol{G}$ is the matrix of the partial derivatives, $\boldsymbol{m}$ $(\Delta x, \Delta y, \Delta z, \Delta \tau)^T$ the matrix containing the changes in the hypocentral parameters required to improve the model fit to the data, $\boldsymbol{d}$ the data vector containing the double differences estimated through Eq. (1) and $\boldsymbol{W}$ a diagonal matrix used to weight equations.

The above system of equations is finally solved by the conjugate gradient algorithm LSQR (Paige and Saunders, 1982) or the singular value decomposition method (SVD), depending on the amount of data. In an iterative way, locations and partial derivatives are updated and data are re-weighted according to the misfit during the inversion and the offset between events. The LSQR method is more efficient with large data sets, as it requires small storage, while SVD is applicable to small data sets and provides reliable estimates of the uncertainty in the relocated parameters.

4. Application

We estimated travel time differences for all the event pairs with a separation distance less than 10 km, at stations located within 500 km from the epicentral area (Fig. 2). In order to optimise the connectivity between events, the original data set was sub-sampled by requiring each event to be connected to a maximum of 10 neighboring events that can be considered as "strong" links. We adopted the typical definition of a "strong" link (Waldhauser, 2001) that includes at least eight phase pairs, one for each degree of freedom.

Although we started with an initial data set of 570 events, our final data, fulfilling the aforementioned requirement, consists of 445 well-connected events that form one large cluster. These events are connected through a network of links that consists of 22,017 P- and 13,728 S-wave phase pairs. The average number of links per event pair is 10, while the average offset between strongly linked events if of the order of 4 km.

The 445 events were relocated by the conjugate gradients method (LSQR, Paige and Saunders, 1982), solving the damped least squares problem. The damping factor damps the differences in the hypocentral locations if the vector difference becomes large or unstable. The choice of the damping factor is rather empirical and depends on the condition of the system to be solved, expressed by the ratio of the largest to smallest eigenvalue (condition number). This ratio is continuously reported during the implementation of the HypoDD code. In our case, a damping factor of 50 was found to be appropriate, resulting in empirically

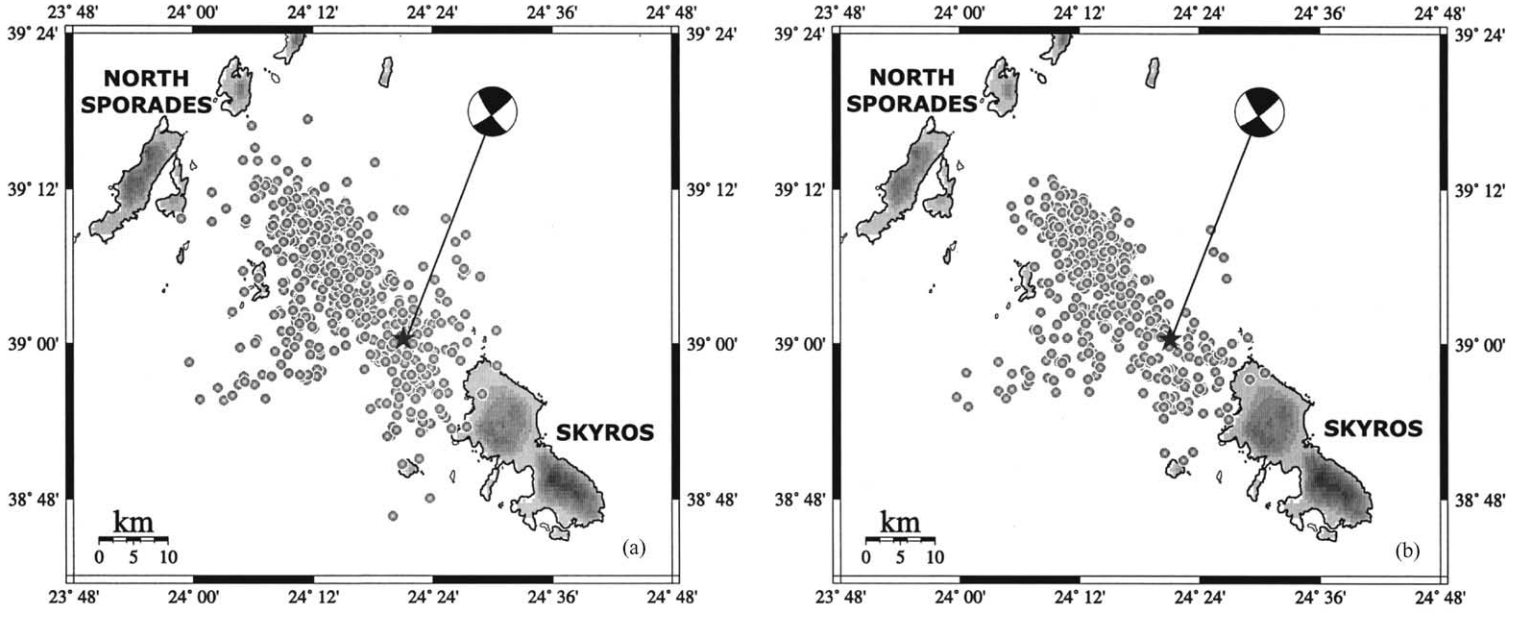

Fig. 3. Map views of the relocated epicentres (b) using double-difference algorithm from catalogue travel time differences and the corresponding epicentres prior to relocation (a).

expected values for the system's condition number (Waldhauser, 2001).

Regarding the weighting of the data, we tested several weighting schemes and found our preferred one by inspecting the relocation results. Our a priori weights, used during the first iterations, are equal to 1.0 and 0.5 for all P- and S-wave observations, respectively. After the first five iterations, we applied a weighting curve that assigns larger weights for small inter-event distances and vice versa, to both the P- and S-phase data (Waldhauser, 2001).

Theoretical travel time differences were estimated based on the 1D P-velocity model (Panagiotopoulos et al., 1985) used for routine earthquake location in the Geophysical Laboratory of the Aristotle University of Thessaloniki. S-wave velocities were estimated from this model, assuming a V_P/V_S ratio of 1.78 (Kiratzi et al., 1987).

Although LSQR is particularly efficient with large sets of data, it does not provide a reliable estimate of the uncertainties assigned to the relocated hypocenters (Waldhauser and Ellsworth, 2000). In order to assess the true uncertainties we also applied the SVD method to a subset of the initial data, which includes 150 earthquakes that occurred within the first 24 h after the mainshock.

5. The relocated aftershocks and their special features

The catalogue with the relocated hypocenter parameters for the 445 relocated events is not listed here but is available upon request. Based on the analysis of a sub-set of our data with the SVD method, the average uncertainty in the new locations is 0.61 km in the E–W direction, 0.71 km in the N–S direction and 0.87 km in the vertical direction. The rms residual decreases from 0.64 s in the initial data to 0.24 s in the relocated catalogue.

Fig. 3 shows the relocated epicentres (part (b) of the figure) and also compares them to the routinely reported ones (part (a) of the figure). The improvement in the location is obvious. There are two clusters of

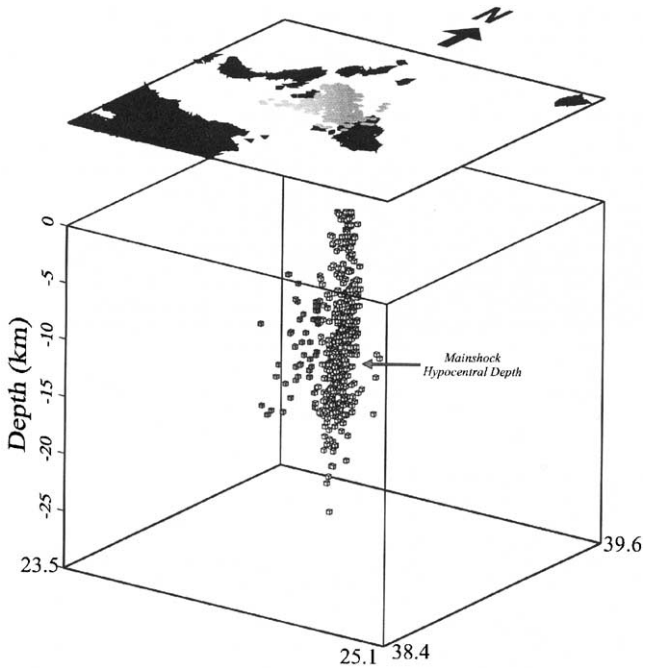

Fig. 4. Three-dimensional views of the relocated hypocenters in a direction perpendicular to the inferred fault strike. The steeply dipping fault plane and the diffused western cluster are clearly shown.

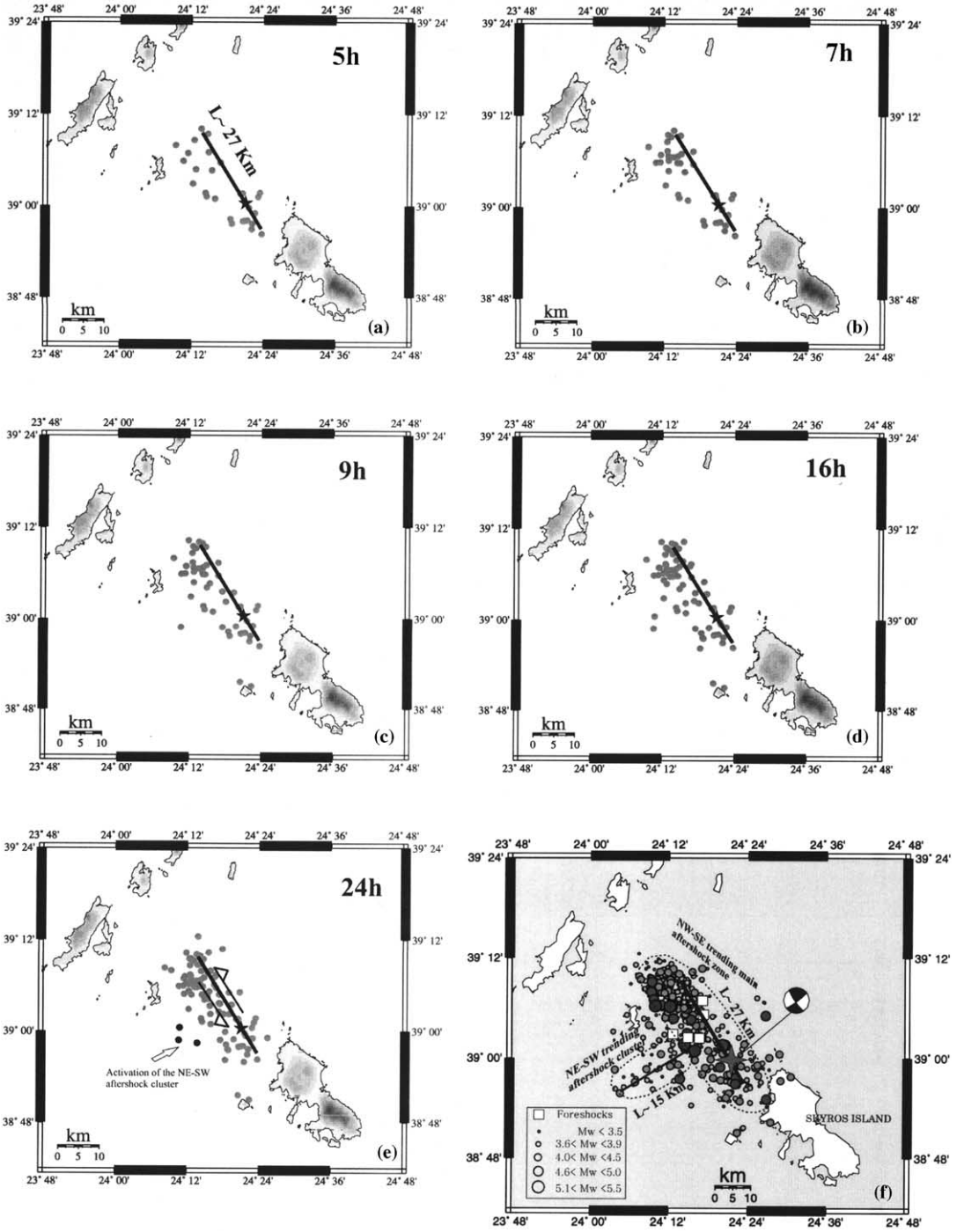

Fig. 5. (a–e) Evolution of the aftershock zone during the first 5–24 h after the mainshock occurrence (time intervals beginning at the mainshock origin time are indicated at the top-right corner of each subplot) used in order to define the fault dimensions. The plots show the activation of the NE–SW trending aftershock cloud after the first 24 h. (f) The full aftershock sequence from 26 July 2001 to 31 August 2001 where the main NW–SE aftershock zone and the diffused NE–SW cluster are shown.

the aftershocks, one well pronounced which forms the main aftershock zone and a spatially smaller cluster orthogonal to the main one. The main aftershock zone has a clear NW–SE trend connected with sinistral shear motion in accordance with the respective plane of the focal mechanism (Benetatos et al., 2002). In this main aftershock zone the larger foreshocks also occurred with epicentres close to the mainshock. The second cluster that is less pronounced trends NE–SW and is associated with the spread of seismicity to nearby faults. The close proximity of the mainshock epicenter to Skyros and the fact that a number of aftershocks occurred on its northern coastland explains the damage observed there compared to the Sporades islands in the north where no serious damage was reported.

In Fig. 4 we present a perspective view perpendicular to the main aftershock alignment (note that the vertical scale is exaggerated). The majority of the hypocenters are concentrated in a narrow zone, delineating the seismogenic fault, which dips steeply towards SW. The scattered seismicity observed off the main hypocenter concentration belongs to the limited cluster at the west of the mainshock epicenter. An interesting observation is a slight change in the dip at a depth somewhere between 5 and 10 km. As a result, the fault appears to be totally vertical near the surface.

In Fig. 5 we compare the evolution of the aftershocks during the first 24 h (insets (a)–(e)) with the entire 5-week-aftershock sequence (Fig. 5f). The fault dimensions are better defined by the aftershocks occurring within the first hour after the mainshock, before the seismicity spreads out around the ruptured during the mainshock area (Mendoza and Hartzell, 1988). Thus, we conclude that the causative fault of the Skyros mainshock had a length of ∼27 km in accordance with what is expected from empirical relations between moment magnitude and fault dimensions applicable to the Aegean Sea area (Papazachos and Papazachou, 1997) and worldwide (Wells and Coppersmith, 1994). Also, Fig. 5a–e indicates that the NE–SW cluster, whose length is 15 km, was not activated simultaneously with the main rupture, but triggered after the occurrence of the Skyros mainshock. Whether this triggering was due to static stress changes or dynamic stresses or even a combination of both processes is hard to tell and is beyond the scope of this paper. Roumelioti et al. (2003) showed that the rupture during the Skyros mainshock propagated bilaterally, even though a small NW directivity component was detected. The fact that the NE—SW trending western cluster of aftershocks is not in the direction of rupture probably indicates the effect of static stress changes rather than dynamic effects.

6. Conclusions and discussion

Hypocentres of the 26 July 2001 Skyros (Greece) earthquake were relocated using the double-difference technique of Waldhauser and Ellsworth (2000). Catalogue data from two Greek Seismological Institutes were combined and processed in order to optimize the connectivity between events. The relocated epicentres revealed clearly the NW–SE striking zone ($L \sim 27$ km) related to the seismogenic fault of the 26 July 2001 mainshock. A more diffused cluster ($L \sim 15$ km) at the western part of the activated area was also detected. Seismicity on this structure was triggered a few hours after the mainshock. Vertical cross sections perpendicular to the main aftershock zone revealed a steeply dipping fault towards SW, in accordance with the focal mechanism of the mainshock (Benetatos et al., 2002).

To our knowledge, this work consists the first implementation of the double-difference technique in the Aegean area. Our results suggest significant improvement (rms residual in the relocated epicentres decreases by a factor larger than 2.5 relative to the preliminary locations) of the seismicity picture in the examined area, although in our relocation we used solely catalogue data. This is very encouraging for future applications of the technique in the wider Aegean Sea area. Supplementary data that may become available in the future, e.g. cross-correlation data, could lead to even more accurate relocations.

Acknowledgements

We thank two anonymous reviewers for constructive comments and suggestions. This work was partially supported by the General Secretariat of Research and Technology of Greece (Ministry of Development).

References

Benetatos, Ch., Roumelioti, Z., Kiratzi, A., Melis, N., 2002. Source parameters of the ***M*** 6.5 Skyros island (North Aegean Sea) earthquake of July 26, 2001. Ann. Geophys. 45 (3), 513–526.

Drakatos, G., Stavrakakis, G., Ganas, A., Karastathis, V., Melis, N., Baskoutas, J., Panopoulou, G., Papis, J., Ziazia, M., Plessa, A., 2002. Preliminary results about the 26 July 2001 Skyros (Aegean Sea, Greece) earthquake and its aftershock sequence. In: Proceedings of the 11th General Assembly of the Wegener Project, June 2002. Athens, CD.

Fréchet, J., 1985. Sismogenèse et doublets sismiques. Thèse d'État, Université Scientifique et Médicale de Grenoble, 206 pp.

Geiger, L., 1910. Herdbestimming bei Erdbeben aus den Ankunftszeiten. K. Ges. Wiss. Gött. 4, 331–349.

Got, J.-L., Fréchet, J., Klein, F.W., 1994. Deep fault plane geometry inferred from multiplet relative location beneath the south flank of Kilauea. J. Geophys. Res. 99, 15375–15386.

Karakostas, V., Papadimitriou, E., Karakaisis, G., Papazachos, C., Scordilis, E., Vargemezis, G., Aidona, E., 2003. The 2001 Skyros, northern Aegean, Greece, earthquake sequence: off-fault aftershocks, tectonic implications, and seismicity triggering, Geophys. Res. Lett. 30 (1), 1012, doi: 10.1029/2002GL015814.

Kiratzi, A., 2002. Stress tensor inversions along the westernmost North Anatolian Fault Zone and its continuation into the North Aegean Sea. Geophys. J. Int. 151, 360–376.

Kiratzi, A., Papadimitriou, E., Papazachos, B., 1987. A microearthquake survey in the Steno dam site in northwestern Greece. Ann. Oeophys. 592, 161–166.

Kiratzi, A., Wagner, G., Langston, C., 1991. Source parameters of some large earthquakes in Northern Aegean determined by body waveform inversion. Pure Appl. Geophys. 135, 515–527.

Louvari, B., 2000. A Detailed Seismotectonic Analysis of the Aegean Sea and the Surrounding Lands Based on the Focal Mechanisms of Small Events. Ph.D. Thesis, Aristotle University of Thessaloniki, 350 pp.

Melis, N.S., Stavrakakis, G.N., Zahradnik, J., 2001. Focal Properties of the $M_w = 6.5$ Skyros, Aegean Sea, Earthquake, Orfeus Newsletter 3, http://orfeus.knmi.nl/newsletter/vol3no2/skyros.html.

Mendoza, C., Hartzell, S.H., 1988. Aftershock patterns and main shock faulting. Bull. Seism. Soc. Am. 78, 1438–1449.

Paige, C.C., Saunders, M.A., 1982. LSQR: sparse linear equations and least squares problems. ACM Trans. Mathematical Software 8 (2), 195–209.

Panagiotopoulos, D.G., Hatzidimitriou, P.M., Karakaisis, G.F., Papadimitriou, E.E., Papazachos, B.C., 1985. Travel time residuals in southeastern Europe. Pure Appl. Geophys. 123, 221–231.

Papadimitriou, E., Sykes, L., 2001. Evolution of the stress field in the northern Aegean Sea (Greece). Geophys. J. Int. 146, 747–759.

Papadopoulos, G., Ganas, A., Plessa, A., 2002. The Skyros earthquake (Mw 6.5) of 26 July 2001 and precursory seismicity patterns in the North Aegean Sea. Bull. Seism. Soc. Am. 92, 1141–1145.

Papazachos, B., Kiratzi, A., Voidomatis, P., Papaioannou, C., 1984. A study of the December 1981–January 1982 seismic activity in northern Aegean area. Bolletino di Geofisica Teorica ed Applicata 101–102, 101–113.

Papazachos, B., Papazachou, C., 1997. The Earthquakes of Greece. Ziti Publications, Thessaloniki, 304 pp.

Papazachos, B.C., Papadimitriou, E.E., Kiratzi, A.A., Papazachos, C.B., Louvari, E.K., 1998. Fault plane solutions in the Aegean Sea and the surrounding area and their tectonic implication. Bolletino di Geofisica Teorica ed Applicata 39, 199–218.

Rocca, A., Karakaisis, G., Karacostas, B., Kiratzi, A., Scordilis, E., Papazachos, B., 1985. Further evidence on the strike slip faulting of the Northern Aegean trough based on properties of the August–November 1983 sequence. Bolletino di Geofisica Teorica ed Applicata 27 (106), 101–109.

Roumelioti, Z., Kiratzi, A., Dreger, D., 2003. The source process of the July 26, 2001 Skyros Island (Greece) earthquake. Geophys. J. Int., in press.

Skarlatoudis, A., 2002. Relocation of Hypocentral Earthquake Parameters in Greece with the Use of Data from Local Experiments and Effects in the Strong Motion Attenuation Relations. M.Sc. Thesis, Aristotle University of Thessaloniki, 120 pp.

Waldhauser, F., 2001. HypoDD—A Program to Compute Double-Difference Hypocenter Locations. US Geological Survey Open-File Report, 113 pp.

Waldhauser, F., Ellsworth, W.L., 2000. A double-difference earthquake location algorithrn: method and application to the Northern Hayward fault, California. Bull. Seism. Soc. Am. 90, 1353–1368.

Wells, D., Coppersmith, K., 1994. New empirical relationships among magnitude, rupture length, rupture width, rupture area, and surface displacement. Bull. Seism. Soc. Am. 84, 974–1002.

Zahradnik, J., 2002. The weak motion modelling of the Skyros island, Aegean Sea, Mw = 6.5 earthquake of July 26, 2001. Stud. Geophys. Geodetica 46, 753–771.